Effect of shot peening on metastable austenitic stainless steels

G. Fargas, J.J. Roa, A. Mateo

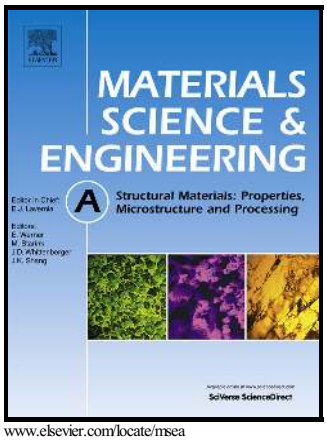

www.elsevier.com/locate/msea

PII: S0921-5093(15)30020-4
DOI: http://dx.doi.org/10.1016/j.msea.2015.05.079
Reference: MSA32407

To appear in: *Materials Science & Engineering A*

Received date: 27 April 2015
Revised date: 13 May 2015
Accepted date: 23 May 2015

Cite this article as: G. Fargas, J.J. Roa and A. Mateo, Effect of shot peening on metastable austenitic stainless steels, *Materials Science & Engineering A,* http://dx.doi.org/10.1016/j.msea.2015.05.079

Effect of shot peening on metastable austenitic stainless steels

G. Fargas[1,2*], J.J. Roa[1,2], A. Mateo[1,2]

[1]CIEFMA - Departament de Ciència dels Materials i Enginyeria Metal·lúrgica. Universitat Politècnica de Catalunya, 08028, Barcelona (Spain)

[2]CRnE, Centre de Recerca en Nanoenginyeria, Universitat Politècnica de Catalunya, 08028, Barcelona (Spain)

[*] Corresponding author, e-mail: gemma.fargas@upc.edu

Abstract

In this work, shot peening was performed in a metastable austenitic stainless steel EN 1.4318 (AISI 301LN) in order to evaluate its effect on austenite to martensite phase transformation and also the influence on the fatigue limit. Two different steel conditions were considered: annealed, i.e., with a fully austenitic microstructure, and cold rolled, consisting of a mixture of austenite and martensite. X-ray diffraction, electron back-scattered diffraction and focus ion beam, as well as nanoindentation techniques, were used to elucidate deformation mechanisms activated during shot peening and correlate with fatigue response. Results pointed out that extensive plastic deformation and phase transformation developed in annealed specimens as a consequence of shot peening. However, the increase of roughness and the generation of microcracks led to a limited fatigue limit improvement. In contrast, shot peened cold rolled specimens exhibited enhanced fatigue limit. In the latter case, the main factor that determined the influence on the fatigue response was the distance from the injector, followed successively by the exit speed of the shots and the coverage factor.

Keywords: Metastable austenitic stainless steels, shot peening; martensitic phase transformation; diffraction, EBSD, FIB.

1. Introduction

Metastable austenitic stainless steels can be considered as TRIP (Transformation Induced Plasticity) steels because plastic deformation, either during forming or under service conditions, can lead to a strain-induced transformation from austenite to

martensite [1]. Two types of martensite may form in austenitic stainless steels: ε and α'. ε-martensite has a hcp crystallographic structure, while α' has a bcc one [2]. The typical transformation sequence can be summarized as $\gamma \rightarrow \varepsilon \rightarrow \alpha'$, where the $\gamma \rightarrow \varepsilon$ transformation has been proposed for austenitic stainless steels deformed under tension, as well as by rolling [3,4]. On the other hand, the direct transformation of austenite into α'-martensite, $\gamma \rightarrow \alpha'$, has been observed too, as found elsewhere [5]. These phase transformations may act as reinforcing mechanisms which make those steels to be candidate materials for the automotive industry, particularly for body-in-white construction, because they combine excellent formability and crash-absorbing capability, together with good corrosion resistance [6].

During service life of a component, fatigue failure may occur. Among a great variety of surface treatments, shot peening is one of the most widely used techniques to increase the resistance of metal parts to fatigue in a large range of industries, such as automotive, aerospace and petrochemical [7,8,9]. It consists of blasting high velocity small beads on the metal component to generate surface hardening and compressive residual stresses which oppose to the nucleation of cracks and also exert a closure effect on those cracks already nucleated, avoiding their propagation [10,11]. Shot peening usually produces detrimental surface effects too, such as increasing roughness, nevertheless it has been shown that the average effect of both beneficial phenomena is more important than those induced by superficial detrimental effects [12,13]. Recent studies [14,15,16], demonstrated that the generation of a nanograined layer over specimens' surface results in a fatigue strength improvement. However, this is true as long as the density and size of surface defects induced by shot peening remain not significant. Otherwise the degradation of the fatigue resistance behavior of excessively shot peened components have been clearly observed [17,18,19].

Numerous investigations have shown the beneficial effects of shot peening on austenitic stainless steels [20,21,22,23,24], describing the role of residual stresses on fatigue life. However, scarce information exists related to metastable austenitic stainless grades. Kleber *et al.* [25] measured the content of martensite induced by shot peening, as a function of depth from the surface, using magnetic Barkhausen noise, while Peyre *et al.* [26] quantified the amount of martensite induced by both conventional shot peening and also laser peening in order to correlate it with the pitting corrosion resistance. In the present work, the relationship between microstructural changes induced by shot peening and fatigue behaviour of the metastable steel was studied. Two different steel conditions

were selected: annealed (with fully austenitic microstructure), and cold rolled (with a biphasic microstructure composed by austenite and martensite). Effect of shot peening was evaluated not only considering the induced martensite but also the influence of the pre-existing martensite produced by cold rolling.

2. Experimental procedure

The experimental material was a commercial AISI 301 LN austenitic stainless steel (corresponding to standard EN 1.4318), supplied as sheets of 1.5 mm in thickness by OCAS NV, Arcelor-Mittal R&D Industry Gent (Belgium). The chemical composition was (in wt. %): Fe-0.03C-17.36Cr-7.18Ni-1.68Mn-0.23Mo-0.55Si-0.14N.

In order to study the influence of the pre-existing martensite on shot peening, a commercial annealed steel (referred as AN) was compared to a cold rolled condition (identify as CR) with a thickness reduction of 40%. Steel in the AN condition displays a fully austenitic microstructure, with an average grain size of 11.7 ± 4.1 μm; while in the CR state, 38 ± 5% corresponds to α'-martensite. Tensile properties and hardness were evaluated for both steel conditions and the results are summarized in Table 1. The presence of martensite on CR specimens leads to an increase of yield stress, ultimate strength and hardness together with a significant reduction of ductility.

Table 1. Mechanical properties and martensite content for the studied steel conditions.

	% α'	σ_{ys} (MPa)	σ_{UTS} (MPa)	A%	HV0.1
AN	< 3	360 ± 10	902 ± 15	42 ± 1	246 ± 8
CR	38 ± 5	1148 ± 16	1173 ± 19	22 ± 2	440 ± 8

Shot peening was conducted using an injector type machine. Stainless steel beads S300, with an average size of 0.3 mm, were used. Their chemical composition was (in wt.%): Fe-1.36Al-17.40Cr-1.14Mn-1.96Mo-9.20Ni-3.40Si. Peening was carried out at two different exit speeds of the shots: 65 and 75 m/s. Two coverages were employed: 200 and 400%. These coverage ratios were obtained by extending the exposure time by a factor of 2 and 4, respectively, with regard to the time required to achieve a complete

coverage, defined as 98% of dimpling of the original surface. The peening processes were done at two different distances from the injector: 700 and 1400 mm.

Surface inspection after the shot peening treatment was performed using light optical microscope with confocal laser scanning mode (CLSM) and field emission scanning electron microscopy (FESEM), together with roughness measurements following the standard EN ISO 16610-21:2012 [27]. The amount of martensite formed due to shot peening was determined by X-ray diffraction using the method corresponding to reference intensity ratio (RIR), according to ASTM E975-03 [28]. This method allows determining the mass fractions of austenite and martensite by using Equation (1):

$$\frac{X_{\alpha'}}{X_{\gamma}} = \frac{RIR_{\gamma}}{RIR_{\alpha'}} \times \frac{I_{\alpha',\,observed}}{I_{\gamma,\,observed}} \times \frac{I_{\gamma,\,reference}}{I_{\alpha',\,reference}} \quad (1)$$

where X_{α} and X_{γ} are the mass fractions of α'-martensite and γ-austenite, respectively; RIR_{γ} and $RIR_{\alpha'}$ are their respective reference intensity ratios; and $I_{observed}$ and $I_{reference}$ are the observed and the reference intensities [29].

The deformed microstructure on the subsurface was analyzed on cross-section specimens through the shot peened region by means of electron back-scattered diffraction (EBSD) operating at 20 kV. Moreover, detailed observations were carried on by a dual beam focused ion beam/FESEM (FIB/FESEM). A thin platinum layer was deposited on the sample prior to FIB machining in order to minimize ion-beam damage. A Ga^{+} ion source was used to mill the surface at a voltage of 5 kV. The final polishing of the cross-sections was made at 500 pA. 3D-FIB tomography was done by collecting around 400 sequential images milled with an ion beam current of 500 pA and reconstructed using AVIZO 8.0 software.

Nanoindentation tests were performed on cross-section peened specimens by using a Nanoindenter XP equipped with continuous stiffness measurements (CSM) modulus. The characterization was performed with a Berkovich tip indenter and the mechanical properties, in terms of hardness and elastic modulus, was analyzed using the Oliver and Pharr equations [30,31]. The indenter shape was carefully calibrated with a fused silica standard sample. Tests were carried on at 100 nm of maximum penetration depth and at a constant deformation rate of 0.05 s^{-1}. Indentations were organized in a regularly spaced array (5 by 300), starting extremely close to the surface on both sides of the

peened specimens. A constant distance between each imprint of 6 μm was kept in order to avoid any overlapping effect.

Flat fatigue specimens with hour-glass shape (Figure 1) were laser machined from the steel sheets with their axis parallel to the rolling direction. As it was shown by the authors in a previous investigation [32], the surface finishing of the sides and corners strongly affects the fatigue results. Thus, it is important to highlight that before fatigue tests, all specimens were grinded and polished at the sides and corners up to achieve the same roughness of the original sheet surface ($R_a = 0.18 \pm 0.02$ μm). The main objective was to avoid premature fracture due to remaining laser cutting defects, in the case of the as-received specimens (AN and CR), and inhomogeneous peened zones for shot peened specimens.

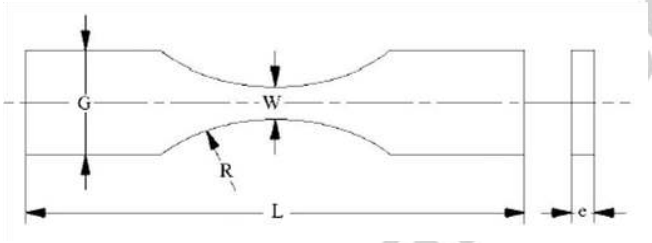

Figure 1. Schematic representation of the fatigue specimens (e = 1.5 mm, G =15 mm, L =95 mm, R = 30 mm and W = 3.8 mm).

Considering that ultimate tensile strengths of AN and CR steel conditions are 880 and 1100 MPa, respectively, a fatigue testing procedure was stated in order to determine the fatigue limit for both conditions. It consisted on starting the tests applying a maximum load (σ_{max}) of 50% of the ultimate tensile strength of the corresponding steel condition and afterwards, if the specimen was able to reach 10^6 cycles without failing, σ_{max} was increased 10%, and so on until fracture, following a staircase method [33]. The value of the fatigue limit was determined using the method proposed by Grove and Campean [34].Tests were conducted under load control mode in a resonant testing machine Rumul Mikroton, working at frequencies around 150 Hz. The imposed stress ratio ($R = \sigma_{min}/\sigma_{max}$) was 0.1. Fatigue tests for shot peened specimens were performed following the same procedure described above.

3.- Results and discussion

Increasing roughness is well-recognized as a side effect of shot peening process. Data on the surface roughness are important for predicting fatigue resistance, as roughen areas might represent local stress concentrations. Figure 2 shows the calculated arithmetic average surface roughness (R_a) based on the definition of ISO 4287 [35]. As it can be observed, the differences in mechanical properties between AN and CR conditions play an important role on their respective surface plastic deformation and as a consequence in the roughness induced by shot peening. In the case of specimens corresponding to annealed condition, the obtained surface is significantly rougher than any of the specimens from cold rolling condition. On the other hand, shot peening performed at short distance from the injector (d = 700 mm) and higher speed (75 m/s) displayed higher roughness, while no significant influence on coverage factor was observed.

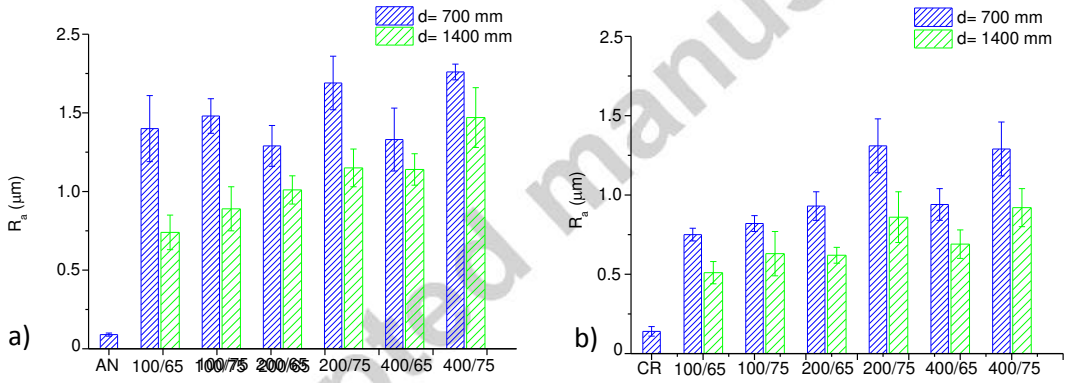

Figure 2. Roughness evolution for the as received and shot peened specimens, considering the two different distances from the injector: 700 and 1400 mm.

X-ray phase analysis was performed in near-surface regions in order to determine the martensite fraction, as depicted in Figure 3. There was a huge difference between both steel conditions. In this sense, AN specimens, with an initial fully austenitic microstructure, displayed a strong increase on martensite content after shoot peening, more than 30% in some cases, while the increment of martensite on CR specimens did not exceed 15%, even under the most critical conditions, i.e., d = 700 mm and 75m/s. Thus, phase transformation developed in a higher degree for softer steel condition (AN), while the higher yield and ultimate strength of CR steel, due to pre-existing α'-martensite, limited the transformation of austenite to martensite. It is important to

highlight that no evidence of ε-martensite was detected by this technique for any of the studied conditions.

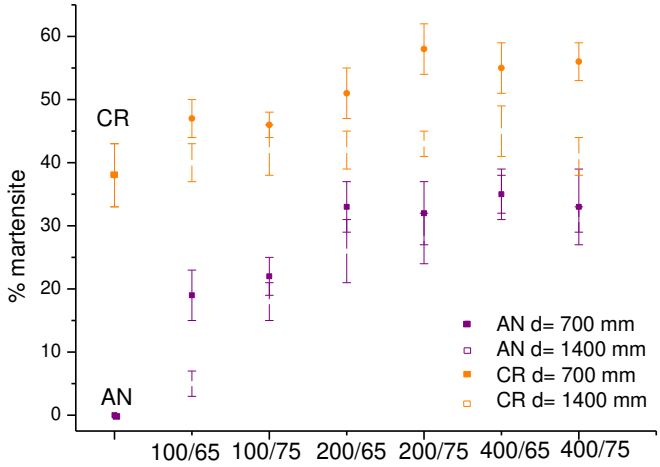

Figure 3. Percentage of martensite for the as received and shot peened specimens.Values in the abscise axis indicate coverage ratio and distance from the injector.

Cross-section analysis on shot peened AN specimens exhibited a deformed austenite microstructure even for 100% coverage factor (Figure 4a). Moreover, it was also possible to identify strain-induced martensite created due to the plastic deformation introduced by the continuous impact of the beads (Figure 4b). Although EBSD performed on CR shot peened specimens showed an increase of martensite for some studied conditions, in agreement with X-ray diffraction results (Figure 3), it was not possible to distinguish the pre-existing martensite from the strain-induced α' as a consequence of shot peening. Furthermore, for this steel condition it was observed that austenitic grains were also extensively deformed with no relevant differences compared to specimens subjected to shot peening.

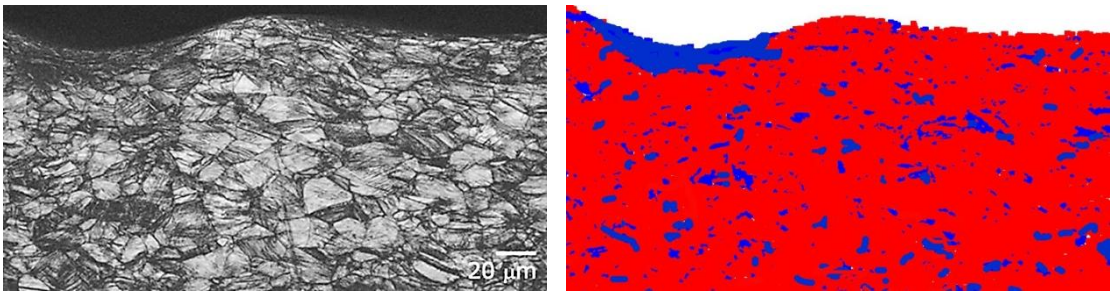

Figure 4. a) Cross-section electron backscattered diffraction (EBSD) map (band contrast) showing the slip bands appearing within the grains in AN shot peened specimen at 65 m/s and d = 1400 mm with a 100% coverage factor, and b) Phase map directly extracted from the EBSD measurements (red: austenitic phase and in blue strain-induced martensite).

A detailed observation of the sub-superficial damage produced by shot peening was performed using FIB for the AN specimens. In order to reveal the microstructure in the trench of interest, the zone of study was exposed to the ion beam during several seconds to produce ion etching and afterwards it was observed by FESEM. Figure 5a shows the austenitic microstructure for the AN specimens in prior to the shot peening, whereas Figure 5b presents a cross section of the same specimen after the shot peening treatment performed at 65 m/s, with d = 1400 mm and 200% of coverage factor. A layer ranging between 0.5 and 1 µm of thickness and consisting of ultrafine-grains can be appreciated in the latter FESEM micrographs. Some authors assumed that such a layer is related to the surface damage during the sample preparation, mainly in the grinding process and the final polishing step, and not with an amorphization effect induced by the Ga^+ ions, [36]. However, in this work, no sample preparation was carried on specimens not even in as-received materials but also after shot peening. Therefore, the formation of those ultrafine-grains should be due to microstructural changes introduced by the high local plastic deformation. This agrees with the results by Uusitalo et al. [37] and Thiriet et al. [38], both working with austenitic stainless steels subjected to attrition peening. Attrition peening is a process based on the same ideas than shot peening, but using ultrasonic vibration in order to peen the surface repeatedly and with multidirectional impacts. Uusitalo et al. [37] reported an ultrafine-grain layer of a thickness around 10 µm for both a stable austenitic steel (AISI 316L) and the same metastable grade used in the present work, i.e., AISI 301LN. A similar layer, although of higher thickness (75 µm), was measured by Thiriet et al. [38] on AISI 316L. Also, several authors

demonstrated that severe plastic deformation (SPD) can induce grain size reductions of several orders of magnitude: pure metals can be refined down to maximum 140 nm [39], dispersion alloys to 50 nm [40] and solid solution alloys to 26 nm [41]. Although shot penning implies less intense surface deformation than attrition peening and also it is not a SPD process, cross-section observations point out that it has produced comparable consequences in the present case. It is important to highlight that the formation of this ultrafine-grain layer was even observed for the cold rolled specimens subjected to shot peened.

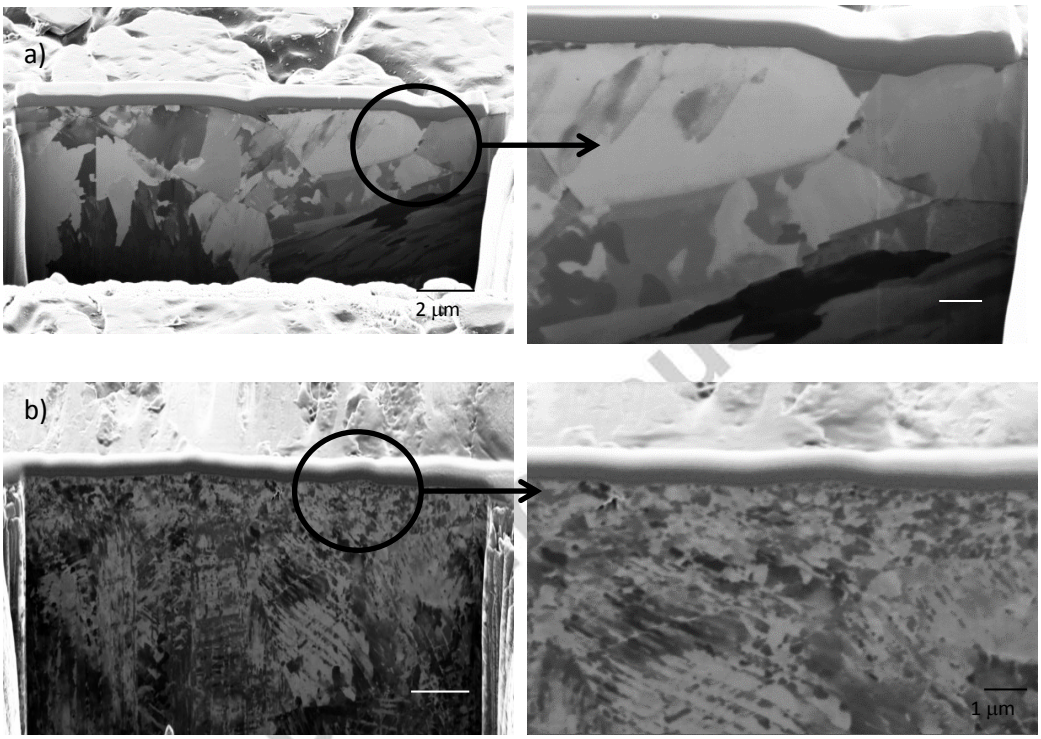

Figure 5. Analysis of the AN subsurface specimens by FIB/FESEM for: a) as received condition, b) after shot peening (65 m/s, d= 1400 mm with a 200% coverage factor).

Figure 6 shows a typical hardness profile of a shot-peened specimen which allows establishing the thickness of the hardened layer. This thickness is defined as the distance from the surface at which hardness values become similar to the bulk material hardness, which is 4.3 ± 0.2 for AN and 5.2 ± 0.3 GPa for CR steel. First values in the profile correspond to the indents placed in bakelite followed by those measured starting at the surface subjected to shot peening until achieving a stabilized hardness level similar to bulk material. It is important to point out that hardness values achieved by nanoindentation are usually higher than those obtained by macroscopic measurements,

i.e. Vickers hardness. This fact is mainly due to differences in definition of the area considered to compute hardness, i.e., projected and contact area, respectively [30,31]. Although significant differences in the hardened layer were observed for AN and CR shot peened specimens, similar maxima hardness values, in the range from 6.8 to 7.2 GPa, were measured for the first 10-15 μm from the surface.

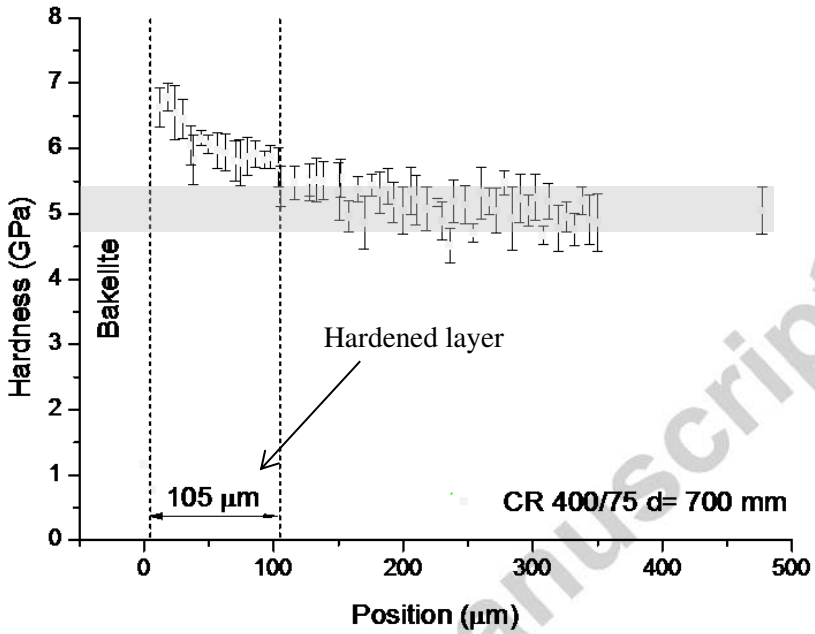

Figure 6. Hardness profile for a CR shot peened specimen where hardness of bulk material is represented as gray colored strip. Each point is the average of three nanoindentation tests. The error bars corresponds to the standard deviation.

Figure 7 plots the thickness of the hardened layer for each studied condition estimated from the nano-hardness profiles. Results point out that both AN and CR steels displayed thicker hardened layer when shot exit speed and coverage were increased. However, the distance from the injector appears as the main factor affecting the thickness. When the shot peening was performed with a low distance (d= 700 mm), thicker hardened layers were obtained. Figure 7b shows that the presence of pre-existing martensite in CR specimens, strengthened the steel in such a way that hardened layer became negligible for shot peened conditions with the longest distance from the injector (d = 1400 mm).

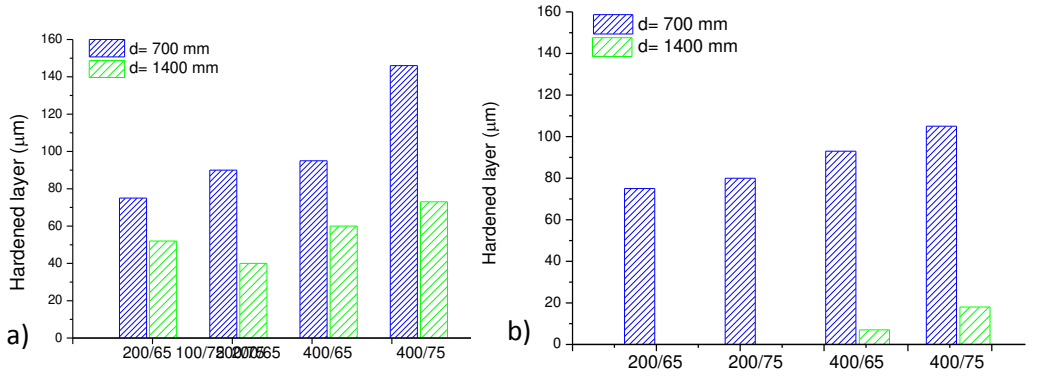

Figure 7. Thickness of the hardened layer of sot peened specimens: a) AN condition; b) CR condition.

The effect of shot peening on fatigue behavior is shown in Figure 8. Normalized fatigue limits (in terms of σ_{max}) of shot peened specimens are represented considering the corresponding value of the steel without shot peening, that were 570 ± 56 MPa for AN and 880 ± 43 MPa for CR. It can be seen that, for AN specimens shot peening influence is practically insignificant. Even for specimens subjected to the higher shot speed (75 m/s) a negative effect on fatigue limit was produced. For those conditions, a surface analysis revealed the presence of large amount of microcracks heterogeneously distributed in the surface, as can be seen in Figure 9.

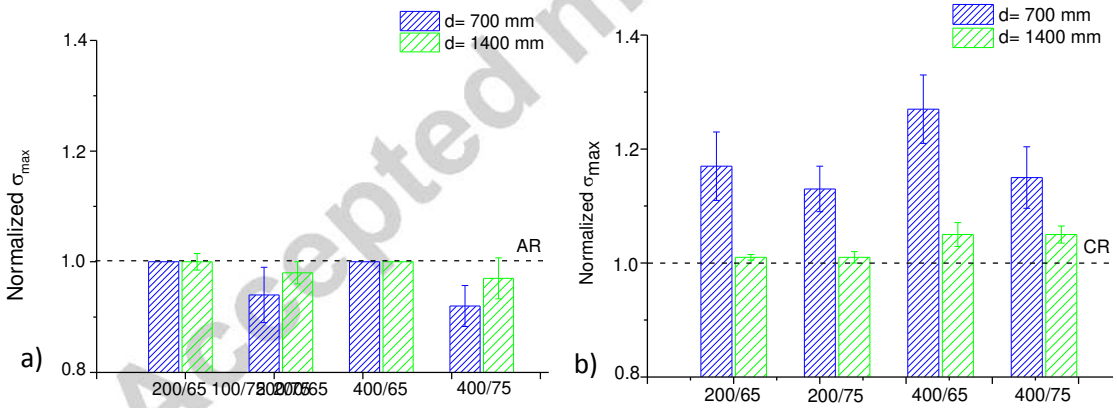

Figure 8. Normalized fatigue limits for shot peened specimens, related to initial steel conditions a) AN; b) CR.

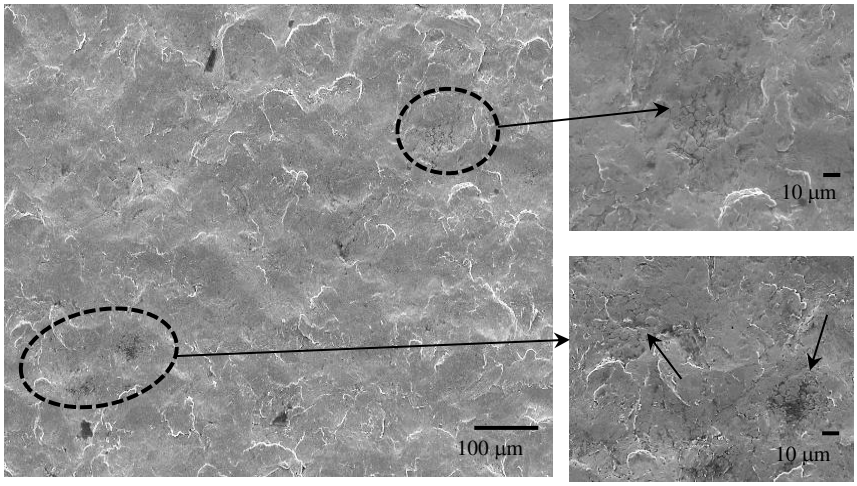

Figure 9. Surface damage observation by FESEM on AR shot peened specimen 75 m/s with a coverage factor of 400 % and 1400 mm distance from the injector.

Attempting to get a more detailed view of the referred damage scenario, FIB cross-sections were conducted in one of these microcracks agglomeration areas discerned in, Figure 10a. Transgranular cracks of several micrometers (1-3 µm approx.) can be observed in the higher magnification image (Figure 10b). 3D reconstruction presented in Figure 10c and supplementary material, allowed to elucidate that microcracks extend throughout the studied zone, around 3 µm, and connect with other microcracks part of the same agglomeration area. It is evident that such scenario is detrimental for the fatigue resistance because the presence of these microcracks, together with the high roughness induced for those "abusive" shot peening conditions, will make easier both the nucleation of fatigue cracks and the initial propagation stage.

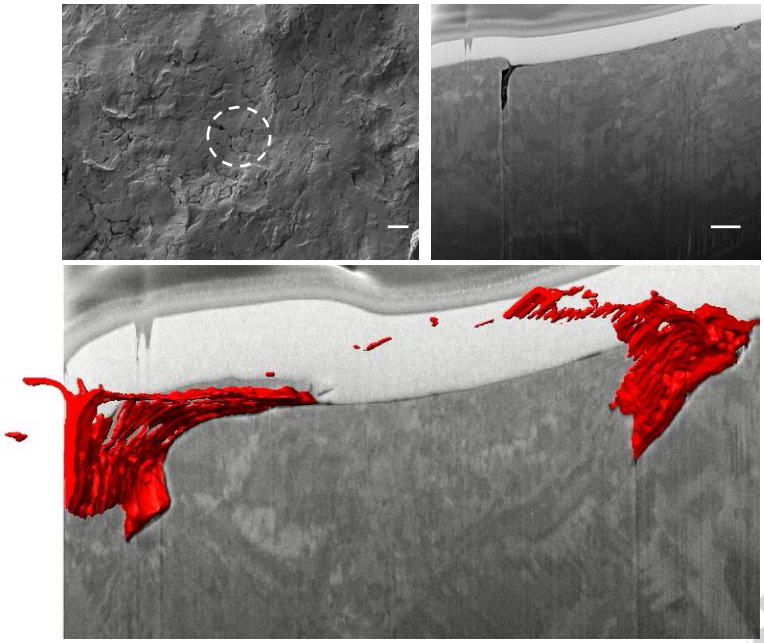

Figure 10. a) FESEM image in which dotted circle indicates the analyzed area by FIB, b) Cross-section image showing microcracking, c) 3D-tomography image obtained after reconstruction of data by collecting around 400 sequential images along 5μm from image b.

Continuing with the analysis of fatigue testing results, Figure 7 reflects that, in contrast to the case of AN samples, noticeable improvements in the fatigue limit were succeeded for specimens corresponding to CR steel, especially at short distance from the injector (d = 700 mm). Particularly, an increase of 30 % in the fatigue limit was achieved when this short distance was combined with a coverage factor of 400 % and a speed of 65 m/s. For these conditions, optimum combination of peening effects was obtained: a thick hardened layer (almost 100 μm), a significant phase transformation to α'-martensite (from an initial 38 % to around 55 %) and also a relatively low roughness (R_a< 1 μm). The important role of roughness is manifested when fatigue limit values for the CR steel after shot peening under the same injector distance and coverage factor, but higher shot speed are considered. Under these conditions, a slightly thicker layer was produced, similar martensite content but higher roughness (R_a~ 1.25 μm), led to a fatigue limit augment of 15%. Surface damage analysis on CR specimens after shot peening, showed smashed particles adhered as a consequence of the repeated contact of the beads, without the presence of microcracks (Figure 11).

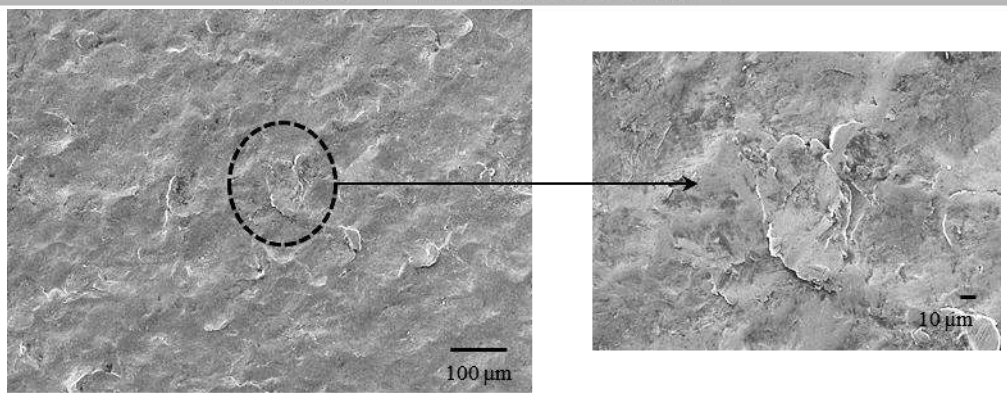

Figure 11. SEM micrograph of CR shot peened specimen at 75 m/s with a coverage factor of 400 % and 700 mm distance from the injector.

4. Conclusions

The effect of shot peening on a metastable austenitic stainless steel was analysed for the same steel grade but considering two pre-existing α'-martensite contents: less than 3% for the annealed condition and 38% for the cold rolled material. The main conclusions resulting from the study can be summarized as follows:

- Shot peening produced higher plastic deformation on the annealed specimens, as a consequence, displayed higher roughness and larger thickness of the hardened layer.
- Extensive austenite to martensite phase transformation was measured for the annealed condition after shot peening, reaching a rise up to 30%. For cold rolled specimens the presence of pre-existing α'-martensite strongly slowed down the proportion of martensite induced by shot peening.
- Cross-section analysis of shot peened specimens performed by FIB revealed the formation of an ultrafine-grain layer of 0.5-1 µm in the near-surface for both studied steel conditions.
- High roughness and microcracks generated during shot peening clearly conditioned the fatigue behaviour of annealed specimens. Therefore, similar or even lower fatigue limits were obtained after shot peening.
- In contrast, the absence of microcracks allowed significant improvements in the fatigue limit for shot peened cold rolled specimens, being the distance from the

injector the most influent parameter, followed in order of importance by the exit speed of the shots and the coverage factor respectively.

Acknowledgements

The authors greatly acknowledge Dr. T. Trifonov "Centre d'Investigació en Nanoenginyeria, CRNE-UPC" for his help in FIB technique. The presented work was carried out within the scope of MAT09-14461 project, supported by the Spanish Ministery of economy. We are grateful to "*Direcció General de Recerca del Comissionat per a Universitats i Recerca de la Generalitat de Catalunya*" for acknowledging CIEFMA as a consolidated Research group (2014SGR). Dr. J. J. Roa would like to thanks the Juan de la Cierva Programme (grant number JCI-2012-14454) for its financial support.

References

[1] J.B. Vogt, Z. Magnin, J. Foct, Fatigue Fract. Eng. Mater. Struct.,16, 1993, pp. 555–564.

[2] H.F.G. de Abreu, S.S. de Carvalho, P.L. Neto, R.P. dosSantos, V.N. Freire, P.M.O. Silva, S.S.M. Tavares, Mater.Res.,10(4), 2007, pp. 359–366.

[3] P.L. Mangonon, G. Thomas, Metall. Trans., 1(6), 1970, pp. 577-586.

[4] V. Seetharaman, P. Krishman, J. Mater. Sci., 16(2), 1981, pp. 523–530.

[5] G. Nolze, Z. Metallkd., 95(9), 2004, pp. 744–755.

[6] R. Andersson, C. Magnusson, E. Schedin., Proc. Conf. of the Second Global Symposium on Innovations in Materials Processing and Manufacturing: Sheet Materials, 2001, TMS, New Orleans (USA), 2011.

[7] D. Clarke, S.S. Birley, The control of Manual Shot Penning, London (UK), 1981.

[8] I. Nikitin, I. Altenberger, Mat. Sci. Eng. A, 465 (1-2), 2007, pp 176-182.

[9] M. Palacios, S. Begherifard, M. Guagliano and I. Fernandez-Pariente, Fatigue Frac. Eng. M, 37(7), 2014, pp. 821-829.

[10] G. Olmi, A. Freddi, Fatigue Fract Eng M, 36(10), 2013, pp. 981-993.

[11] M. Newby, M.N. James, D.G. Hattingh, Fatigue Fract Eng. M., 37(7), 2014, pp. 706-716.

[12] E.R. de los Rios, M. Trull, Fatigue Fract. Eng. Mater. Struct., 23, 2000, pp. 709-716.

[13] M. Guagliano, L. Vergani, Eng. Fract. Mech., 71, 2004, pp. 501-512.

[14] K. Miková, S. Bagherifard, O. Bokuvka, M. Guagliano, L. Trsko, Int. J. Fatigue, 55, 2013, pp. 33-42.

[15] L. Trsko, M. Guagliano, O. Bokuvka, F. Novy, Proc. Eng, 74, 2014, pp. 246-252.

[16] S. Bagherifard, I. Fernandez-Pariente, R. Glelichi, M. Guagliano, Int. J. Fatigue, 65, 2014, pp. 64-70.

[17] R. Fathallah, A. Laamouri, H. Sidhom, Int. J. Fatigue, 26 (10), 2004, pp. 1053-1067.

[18] R. Fathallah, H. Sidhom, C. Braham, L. Castex, Mater. Sci. Technol., 19, 2003, pp. 1050-1056.

[19] U. Martin, I. Altenberger, B. Scholtes, K. Kremmer, H. Oeteel., Mater. Sci. Eng. A, 246, 1998, pp. 69-80.

[20] S. Wang, Y. Li, M. Yao, R. Wang, J. Mat. Proces. Technol., 73, 1998, pp. 64-73.

[21] M.A.S. Torres, H.J.C. Voorwald, Int. J. Fatigue, 24, 2002, pp. 877-886.

[22] P.K. Brahmankar, S.B. Mahagaonkar, C. Y. Seemikeri, Conf. Proc. ICSP-10, Tokyo (Japan), 2010.

[23] K. Dalei, B. Karlsson, Int. J. Fatigue, 38, 2012, pp. 75-83.

[24] M. Ali Terres, N. Laalai, H. Sidhom, Mater. Design, 35, 2012, pp. 741-748.

[25] X. Kebler, S. Pirfo Barroso, Mat. Sci. Eng. A, 527, 2010, pp. 6046-6052.

[26] P.Peyre, X. Scherpereel, L. Berthe, C. Carboni, R. Fabbro, G. Béranger, C. Lemaitre, Mat. Sci. Eng. A, 280, 2000, pp. 294-302.

[27] EN ISO 16610-21:2012: Geometrical product specifications (GPS). Filtration. Part 21: Linear profile filters: Gaussian filters (ISO 16610-21:20111)

[28] ASTM E975-03. Standard Practice for X-Ray Determination of Retained Austenite in Steel with Near Random Crystallographic Orientation. ASTM Internacional, 2003.

[29] ASTM E 975-03. Standard Practice for X-Ray Determination of Retained Austenite in Steel with Near Random Crystallographic Orientation. ASTM Internacional, 2003.

[30] W. C. Oliver, G. M. Pharr., J. Mater. Res., 7, 1992, pp. 1564-1583.

[31] W. C. Oliver, G. M. Pharr. J. Mater. Res., 19, 2004, pp. 3-20.

[32] A. Mateo, G.Fargas, J. Calvo, J.J. Roa, Mat. Test., 57(2), 2015, pp. 1-5.

[33] A.M. Mood, W.J. Dixon, J. Am. Statist. Assoc., 43(241), 1948, pp. 109-126.

[34] D. Grove and F. Campean, Test, 24, 2008, pp. 485-497.

[35] ISO 4287:1997: Geometrical Product Specifications (GPS) - Surface texture: Profile method -- Terms, definitions and surface texture parameters.

[36] J. J. Roa, G. Fargas, E. Jiménez-Piqué, A. Mateo, Mat. Sci. Eng. A, 597, 2014, pp. 232-236.

[37] J. Uusitalo, L. P. Karjalainen, D. Retraint, M. Palosaari, Mat. Sci. For., 604-605, 2008, pp. 239-248

[38] T. Thiriet, T. Czerwiec, D. Hertz, G. Marcos, T. Duchanoy, S. Migot, B. Brugier, M. Foucault, T. Belmont, Defect and Diffus. Forum, 323-325, 2012, pp. 471-476.

[39] A.P. Zhilyaev, J. Gubicza, G. Nurislamova, A. Révész, S. Surinach, M.D. Baro, Phys Status Solidi, 198, 2003, pp. 263–271.

[40]T. Ungar, G. Tichy, J. Gubicza, R.J. Hellmig, Powder Diffract, 20, 2005, pp. 366–375.

[41] P.V. Liddicoat, X.Z. Liao, Y. Zhao, Y. Zhu, M.Y. Murashkin, E.J. Lavernia, Nat Commun, 1, 2010, pp. 63-69.